CELLULOSE/WOLLASTONITE BASED GREEN MEMBRANES USING RICE STRAW: FABRICATION AND CHARACTERIZATION

JAVAD MOKHTARI[*,**] and MOTAHAREH KANAFCHIAN[**]

[*]*Department of Polymer Engineering and Color Technology, Amirkabir University of Technology (Tehran Polytechnic), Iran*
[**]*Department of Textile Engineering, Faculty of Engineering, University of Guilan, Guilan, Iran*
✉ *Corresponding author: J. Mokhtari, j.mokhtari@guilan.ac.ir*

Received January 8, 2022

Cellulose/wollastonite membranes were prepared with an environmentally friendly process using N-methylmorpholine-N-oxide (NMMO), which resulted in mesoporous membranes with slit-shaped pores. Cellulose and wollastonite were extracted from rice straw with different methods. Some parameters, such as weight ratios of cellulose and wollastonite in solution, concentration, thickness of the cast solution on the support layer and porosity of the support layer, influence the formation of the porous cellulose/wollastonite membrane. It was concluded that the porosity and pore size of the cellulose/wollastonite membrane decreased with lower cellulose and higher wollastonite amounts. The membranes became more brittle by increasing the amount of wollastonite, while pure cellulose membranes did not have enough strength to be placed on the polyester support layer. Also, the concentration of cellulose should not be too high or too low. The thickness of the cast solution on the support layer should not be too high, as it reduces the porosity; on the other hand, low thickness reduces the performance of the membrane.

Keywords: membrane, rice straw, cellulose, wollastonite

INTRODUCTION

Rice straw is an important by-product resulting from harvesting crops. Due to an increase in people's environmental awareness, more and more researchers are investigating the comprehensive utilization of rice straw and other waste biomass resources. Typically, rice straw is burned in the fields, causing local and regional air pollution problems. Straw burning releases particulate matter into the atmosphere, which is associated with air pollution and human respiratory ailments. The release of toxic substances into the environment, such as carbon monoxide (CO), black carbon from straw burning, heavy metal loads in water and soil, *etc*., is identified as causing human toxicity. Toxic substances accumulate in vegetables, fruits, meat, milk and other animal products, which, in turn, are ingested by humans.[1] Thus, recovering straw wastes is very important for preventing environmental pollution.

As known, rice straw is mainly composed of cellulose (40–50%), hemicelluloses (20–30%) and lignin (10–18%), cellulose being trapped in the hemicellulose-lignin matrix, which makes its separation extremely difficult. Moreover, a complex hydrogen bond network exists among the cellulose molecules; thereby, cellulose is insoluble in common solvents. At present, inorganic acid-base cooking and organic solvent extraction are the major methods for extracting cellulose from crop straw.[2]

Cellulose can exist in at least 5 allomorphic forms[3] and possesses strong hydrogen bonds due to the presence of the three hydroxyl groups on the cycle. This key feature gives it high resistance towards ordinary organic solvents (methanol, ethanol, butanol, acetone, tetrahydrofuran (THF), acetonitrile) and water.[4] Therefore, cellulose should be considered as a potentially great material for membranes. This lack of solubility makes it harder to cast a solution containing cellulose, but at the same time, it gives cellulose membranes strong stability. This key property, in addition to its biodegradability, enables cellulose to meet high expectations when applied to filtration. Other advantages of cellulose membranes are their relatively low cost, good compatibility with biological compounds and excellent hydrophilic properties.[5]

Wollastonite ($CaSiO_3$) is largely inert and has a polymorph structure, either α-wollastonite (pseudowollastonite), or β-wollastonite.[6-8] Wollastonite changes to pseudowollastonite at 1125 °C, and congruently melts at 1544 °C.[9] Calcium silicate hydrates are transformed into β-wollastonite by annealing in the temperature range from 800 °C to 1150 °C.[10]

Various raw materials have been used to synthesize wollastonite ($CaSiO_3$), derived from chemical or mineral precursors, to produce an end product with significant purity and good mechanical properties.[11] Previous studies have successfully synthesized wollastonite using chemicals and minerals, such as fumed silica, commercial silica, silica sand and sodium silicate as the precursor for silica. Silica can be derived from rice straw ash.[6,12-16] Rice straw ash has been widely used as a biomass resource, animal feed, biosorbent and as bioethanol, in the effort to better manage this by-product.[11] However, there are fewer studies concerning the use of rice straw ash for biomaterial purposes, compared to those about rice husk ash.[17-19] In recent years, wollastonite has been widely used in cements and ceramics due to its strength, low shrinkage, lack of volatile constituents, and body permeability, as well as its fluxing characteristics.[20] Furthermore, wollastonite is also widely applied in the biomaterials field, owing to its bioactivity and degradability. Calcium silicate has been proven to be an extremely good material for *in-vitro* bioactivity.[21]

NMMO (N-methyl morpholine-N-oxide) has a strong electronegative oxygen atom that can break the hydrogen bonds between cellulose chains; as a result, new hydrogen bonds are formed with NMMO to produce a viscous solution of cellulose.[22-24] The particular characteristic of the NMMO process is that it involves essentially physical phenomena, so that no chemical reaction takes place and no chemical by-products are formed, which avoiding the problem of their disposal as waste products or the need to transform them back into the initial substances by chemical methods.[25,26] The use of NMMO as a new organic solvent for cellulose opens up new perspectives for cellulose membrane development and its application in separation processes.[5]

Porous membranes consist of a solid matrix with defined holes or pores, which have diameters ranging from less than 2 nm to more than 20 mm.[27] The separation of solutes by porous membranes is mainly a function of molecular size and membrane pore size distribution.[28] These membranes are used to separate colloid particles or large molecular weight solutes from the solvent. High selectivity can be obtained when the solute size or particle size is relatively larger than the pore size of the membrane. Using the definition of pore size as adopted by the IUPAC,[29] the porous membrane with average pore diameters larger than 50 nm is classified as macroporous, and those with average pore diameters in the intermediate range between 2 and 50 nm are classified as mesoporous. Membranes with average pore diameters between 2 and 0.2 nm are classified as microporous. Below 0.2 nm, membranes are classified as nonporous (or dense).

The techniques commonly used for preparation of polymeric membranes include phase inversion, sintering, stretching, track etching, and template leaching. The phase inversion process can be described as a mixing process, whereby the initially homogeneous polymer solution is transformed in a controlled manner from a liquid to a solid state. Polymer precipitation can be accomplished in several ways, namely by immersion precipitation (or non-solvent induced phase separation), thermal precipitation (or thermally induced phase separation), precipitation by solvent evaporation and precipitation from vapor phase. Thus, the phase inversion technique can be used to produce porous membranes with a large variety of pore size by varying the type of polymer, polymer concentration, composition of cast solution, precipitation medium, and precipitation temperature. Table 1 summarizes membrane processes based on macroporous, mesoporous, and microporous membranes and their separation mechanism and transport model.[30]

Related to this, Feng *et al*.[31] studied the preparation of a rice straw-based green separation layer for efficient and persistent oil-in-water emulsion separation**.** A low-cost and eco-friendly separation layer with a rough structure and rich anionic groups was fabricated from rice straw (RS) via a simple acid-base treatment and slight squeeze process.

The purpose of the present work is to extract cellulose and wollastonite from rice straw and use them in the development of membranes by an environmentally friendly process with the NMMO solvent. The effects of preparation parameters, such as weight ratio of cellulose and wollastonite in the mixture solution, solution concentration, thickness of the cast solution on the support layer, on the pores size and other properties of the cellulose/wollastonite membrane were examined.

Table 1
Overview of membrane processes based on membrane pore size and transport model[29]

Process	Type of membrane	Applied driving force	Separation mechanism/ mode of transport
Microfiltration	Macroporous	Hydrostatic pressure	Size exclusion, convection
Membrane distillation	Macroporous	Temperature difference partial pressure gradient	Diffusion
Ultrafiltration	Macroporous, Mesoporous	Hydrostatic pressure	Size exclusion, convection
Nanofiltration	Mesoporous	Hydrostatic pressure concentration gradient	Size exclusion, electrostatic interactions, solution/diffusion
Dialysis	Microporous	Concentration gradient	Diffusion
Gas separation	Microporous (Or dense)	Hydrostatic pressure concentration gradient	Knudsen diffusion (solution/diffusion)

EXPERIMENTAL

Extraction of cellulose from rice straw

Rice straw was obtained from a local source (Guilan, Iran). Dried rice straws, with 4–5 cm length, were soaked in 17.5 wt% NaOH solution (sodium hydroxide powder purchased from Merck) for 2 h, and then the fibers were washed with distilled water to neutralize the pH. In order to remove the hemicelluloses, pectin and semi-crystalline regions, the fibers were hydrolyzed with HCl (2M) solution (hydrochloric acid purchased from Merck) at 80 °C for 2 h and washed with distilled water for several times. The acid hydrolyzed pulp was treated with 2 wt% NaOH solution at 80 °C for 2 h to remove the remaining hemicelluloses and soluble lignin. The alkali treated fibers were washed repeatedly. The stock was bleached by a 20 wt% $NaClO_2$ solution at 50 °C for 1 h to remove the insoluble lignin.[32,33]

The liquid was removed by filtering to separate pure cellulose. The cellulose was washed with distilled water until neutralization.[34] Acid hydrolysis of rice straw was conducted according to the method of Battista.[35] Forty grams of extracted cellulose was hydrolyzed in 1000 mL of 2.5N hydrochloric acid at 100 °C for 30 min with constant agitation. The reaction mixture was allowed to cool at room temperature and filtered. The white residue obtained was washed repeatedly with distilled water until it became acid-free (the filtrate showed a near neutral pH). The residue was then dried in a vacuum oven to constant weight for 5 h at 70–80 °C and ground to fine powder afterwards. Figure 1 shows parts of this process.

Synthesis of wollastonite ($CaSiO_3$) from rice straw ash (RSA)

The preparation of wollastonite from the agricultural waste was carried out by following a previously described procedure.[36] Rice straw collected from the field was washed, and treated with HCl (1N) in boiling conditions and washed with distilled water; the pH was adjusted to neutral. The resultant was calcined at 550 °C up to 5 h to obtain white silica ash. A predetermined amount of white rice straw ash was dissolved in 0.8M of NaOH solution in boiling condition; finally, the resultant sodium silicate was obtained. Equimolar amounts of calcium nitrate and sodium silicate were mixed to obtain a clear white precipitate. The precipitate was washed several times with deionized water and ethanol, then centrifuged and dried at 60 °C to obtain wollastonite.[37] Figure 2 shows parts of this process.

Preparation of cellulose/wollastonite solution

First, a 15 wt% cellulose solution was prepared by the N-methyl morpholine-N-oxide (NMMO) method (NMMO monohydrate purchased from Sigma-Aldrich). Cellulose and NMMO monohydrate were stirred at 70 °C (melting point of NMMO monohydrate) until NMMO started to melt. Then, 70 °C water was added to the mixture powder over a period of 1 h under stirring, using a magnetic stirrer at 4000 rpm. Then, wollastonite was added to the solution. The mixing of the polymer solution was finished when the solution became clear. The cellulose/wollastonite solution was prepared in 50/50, 70/30 and 90/10 weight ratios.

Figure 1: Cellulose extraction process from rice straw

Figure 2: Wollastonite preparation process from rice straw

Figure 3: Preparation of membrane by an automatic film coater doctor blade

Preparing cellulose/wollastonite membranes on nonwoven polyester

For preparing the membrane, an MTI-20-32 doctor blade (China) was used. Doctor blading was performed on nonwoven polyester, which was used as a support for the substrate. The solution was cast on nonwoven layers with 4 different thicknesses: 20, 50, 100 and 500 μm (Fig. 3). The coated membranes were dried in an oven at 60 °C for 4 h.

RESULTS AND DISCUSSION

Fourier-transform infrared spectroscopy

The FTIR spectra of all the samples (cellulose, wollastonite and cellulose/wollastonite film) are presented in Figure 4. A broad peak around 3478 cm^{-1} due to stretching vibration of the O-H bond was observed in cellulose, while peaks due to C-H bond stretching frequency were detected at 2915 cm^{-1}. Owing to the increased cellulose content and decreased lignin and hemicellulose portions of the raw biomass, these peaks appeared sharper. A diffused peak at 1638 cm^{-1} was due to the adsorbed moisture and indicated cellulose–water interaction. Also, the C-H vibration of the glycosidic bond was observed at 1383 cm^{-1} and 1164 cm^{-1}, while the peak due to C-O-C glycosidic bond vibration (pyranose C-O-C ring stretching) appeared at 1060 cm^{-1}. The peak at 896 cm^{-1} was due to C-H rocking vibrations and could be correlated to the purity of the cellulose structure.[38]

The absorption bands visible at wavelengths of 2915.49–3478.58 cm^{-1}, 1430.74 cm^{-1}, 1383.83 cm^{-1} and 1060.26 cm^{-1} were associated with tensile vibrations of the O–H and C–H groups, flexural and modified vibrations of the C–H group, and flexural vibrations of the C–O group, respectively. The absorption bands recorded for the pure cellulose were observed in the FTIR spectrum of the prepared cellulose/wollastonite membrane as well.[39]

The FT-IR spectra of the wollastonite shows a broad band in the region of 3462.46 cm^{-1} and 1792.15 cm^{-1} by the stretching and the bending vibration of O–H groups due to the moisture content of the sample. The peak at 873.87 cm^{-1} was due to the CO_3^{2-} ions of $CaCO_3$.The broad band at 1086.10 cm^{-1} was observed due to the formation of amorphous silica. This indicates the formation of a calcium carbonate phase and amorphous silica after the combustion process. The spectrum did not display the

bands at 868 cm^{-1} after calcination and 1381 cm^{-1}, which shows that calcium carbonate and amorphous silica got converted into single-phasic wollastonite. The bands occurred in the region of 1086.10 cm^{-1}, which was attributed to the Si–O–Si stretching vibration, and 873.87 cm^{-1}, which was due to Si–O–Ca groups. The band near 470.15 cm^{-1} was due to the rocking vibration of the Si–O bond.

The strong peaks in Figure 4 (b) indicate single phasic wollastonite, without any secondary phases.[40] The intense bands at 712.64 and 470.15 cm^{-1} correspond to Si-O^- and SiO_4^{4-}, while the absorption band at 1792.15 cm^{-1} can be assigned to the vibration mode of the Si-O-Si bond. The absorption band at 873.87 cm^{-1} represent Si-CH_3 functional groups. The band between 1340-1260 cm^{-1} is associated with the Si- CH_3 and SiO_4^{4-} functional groups or Si-O^- stretching.[41]

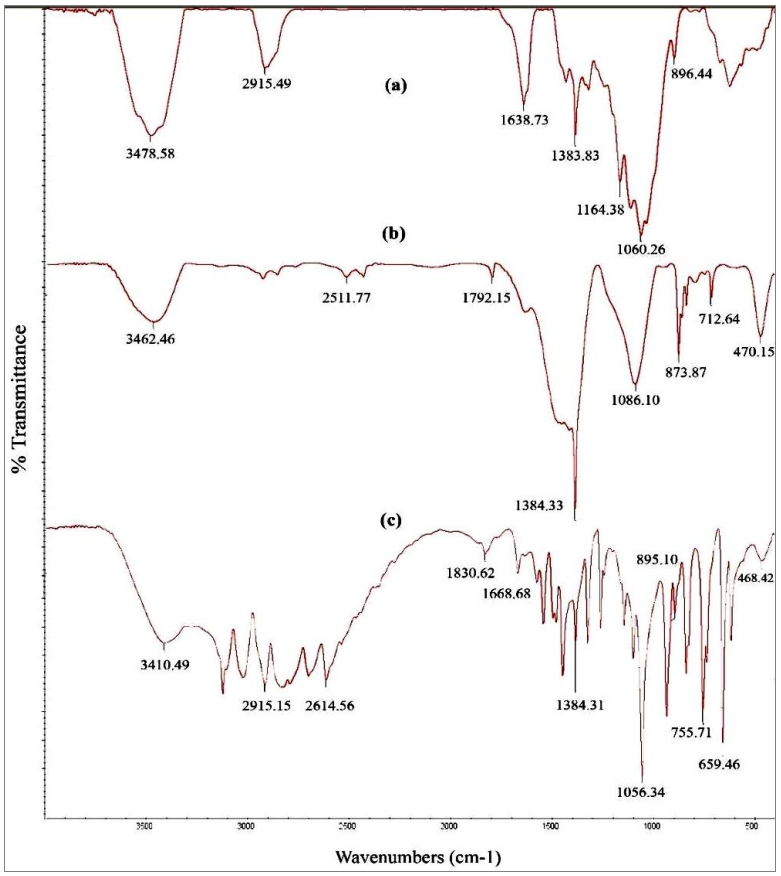

Figure 4: FTIR spectra of (a) cellulose, (b) wollastonite and (c) cellulose/wollastonite membrane

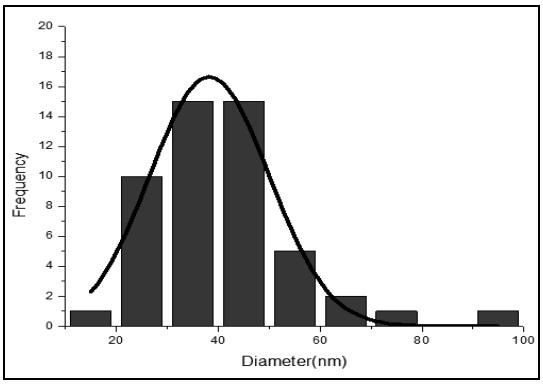

Figure 5: Frequency-diameter (nm) histogram for cellulose powder

Measurement of cellulose powder size

The size of the cellulose powder was measured by SEM. 50 particles of cellulose powder were randomly picked and examined in terms of diameter. Then, a histogram was plotted (Fig. 5) for

frequency-diameter (nm). As can be seen from the diagram, the diameter of 40 nm was the most frequent one. The mean diameter of the cellulose powder is 40 nm.

Scanning Electron Microscopy (SEM)

Scanning electron microscopy is useful to focus on the characterization of membrane structure. Since polymeric membranes are not conductive, they need to be coated before the imaging, but still low electron contrast prevents high magnification images.

Figure 6 shows SEM images of pure cellulose membranes with different thickness: 500, 100, 50, 20 μm, cast on polyester backing. The thickness of 100 μm was selected as it allowed the best covering, without frangibility.

Figure 7 shows images of the cellulose/wollastonite membranes with different ratios: 90/10, 70/30, 50/50, with 100 μm thickness, cast on the polyester support layer. A more porous structure can be seen in Figure7 (A) for the cellulose/wollastonite membrane with 90/10 ratio. This indicates that using a lower percentage of wollastonite results in a more porous membrane. The membrane porosity was also investigated by BET analysis. The membranes become more brittle with an increasing amount of wollastonite, while pure cellulose membranes do not have enough strength to be placed on the nonwoven polyester support layer.

Figure 8 shows cross-sectional views of the 90/10 cellulose/wollastonite membrane, with 100 μm thickness, cast on the polyester support layer. These images confirm the uniformity of the cellulose/wollastonite membrane on the polyester layer.

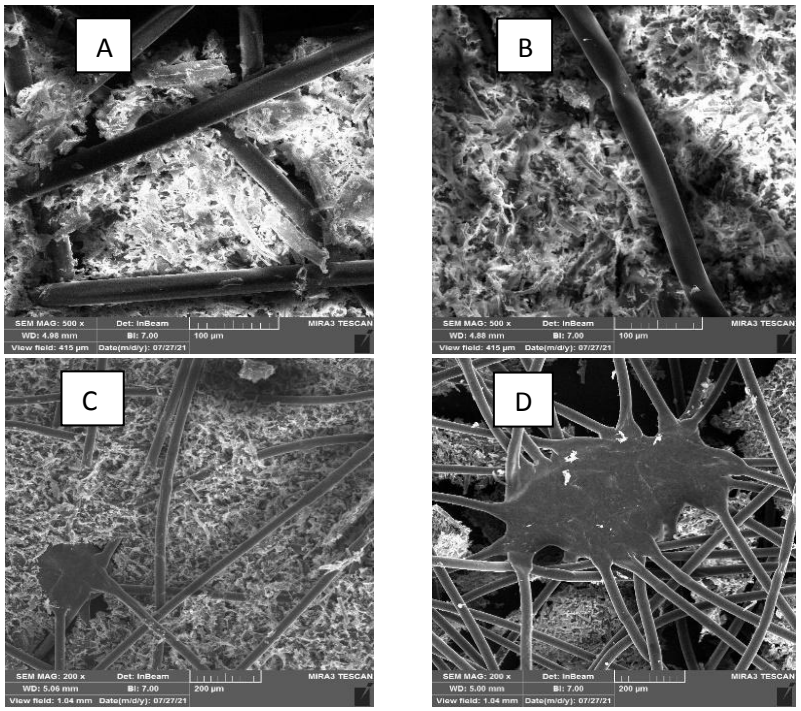

Figure 6: Pure cellulose membranes with different thickness: A) 500 μm, B) 100 μm, C) 50 μm, and D) 20 μm, cast on polyester backing

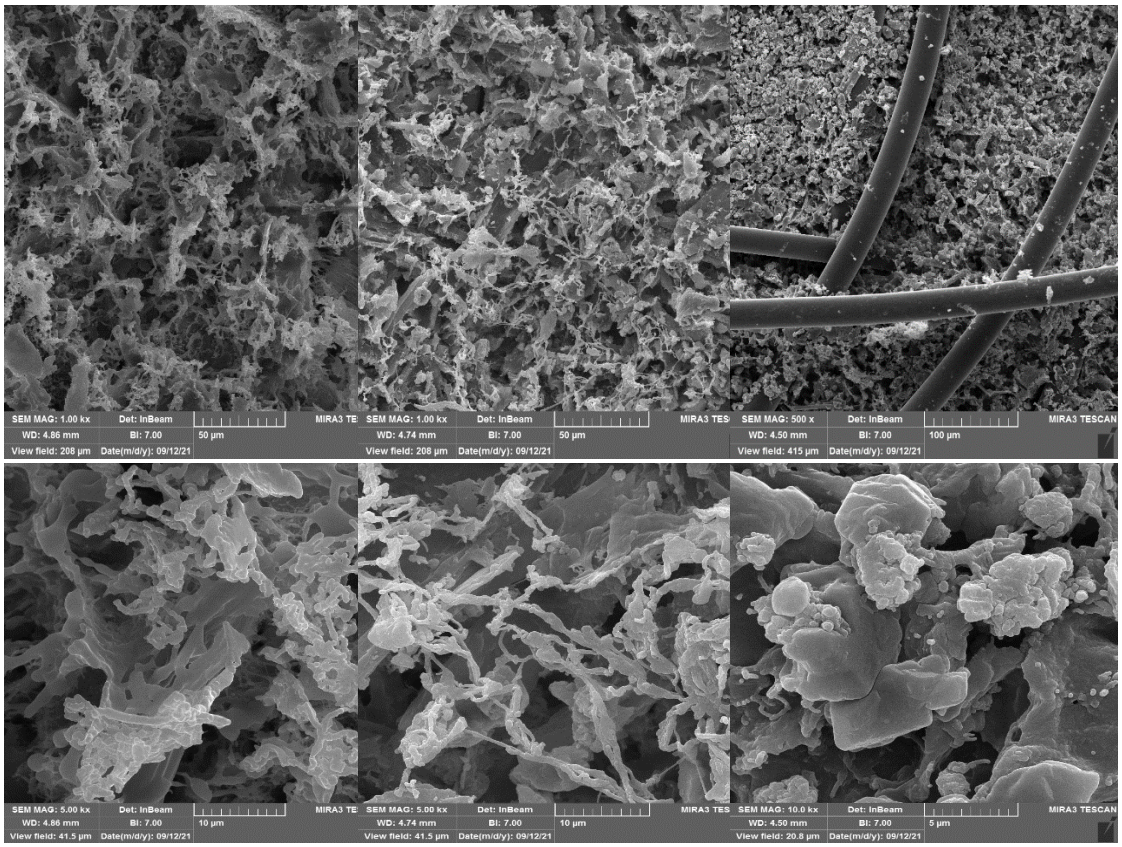

(A) (B) (C)

Figure 7: Cellulose/wollastonite membranes with different ratios: (A) 90/10, (B) 70/30 and (C) 50/50, with 100 µm thickness, cast on polyester support layer

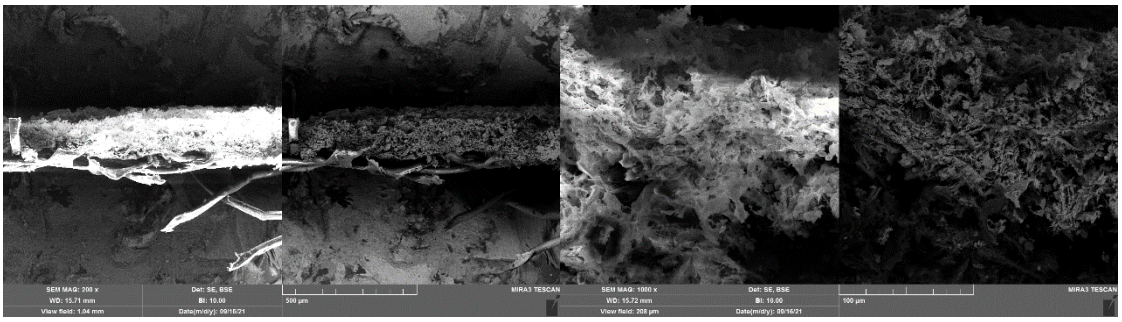

Figure 8: Cross-sectional views of 90/10 cellulose/wollastonite membrane with 100 µm thickness, cast on polyester support layer

Brunauer Emmett Teller analysis (BET)

One of the techniques used to measure the porosity of membranes is gas adsorption/desorption analysis. Nitrogen adsorption/desorption isotherms for Brunauer−Emmett−Teller (BET) surface area determination were obtained using a BELSORP MINI II instrument. It has a molecular pump and increases the vacuum to 10^{-6} Pascal. The pressure resolution in this device is up to 4 Pascal. The vacuum rate is between 1 and 500 milliliters per minute and the controlled pressure spread is 1 meter per kilopascal. The samples were degassed for 5 h at 100 °C under high vacuum to remove any adsorbed species before nitrogen adsorption analysis.

The surface area and pore size of porous materials can be measured by this technique. Generally, nitrogen is used as condensable gas at its boiling point and the volume of adsorbed gas is recorded at various vapor pressures. The data is drawn from the adsorption isotherm (amount of gas adsorbed versus relative pressure) and analyzed by assuming capillary condensation. The Brunauer–Emmett–Teller (BET) theory is mostly used to explain the physical adsorption of gas molecules on the surface of a solid material. According to this theory, the monolayer molecular adsorption (Langmuir theory) is

extended to multilayer adsorption by assuming that gas molecules adsorb infinitely and the layers have no interaction between each other, while the Langmuir theory is applicable to each separate layer.

In the present study, when the drying/degassing process before the BET analysis was not successful, no data was recorded for long time taking experiments. After several attempts, drying and degassing at 100 °C for 5 hours was selected as the optimum treatment before BET analysis.

The volume of micropores and mesopores is measured using the T-plot mode and the distribution of cavities in mesopores is studied by the BJH method (method of Barrett, Joyner and Halenda). Figure 9 (A-D) shows various modes of analysis, namely, adsorption/desorption isotherm, BET plot, T plot and BJH plot, respectively, while Table 2 presents the values obtained from porosity analysis. The pore shape can be roughly approximated by any of the following three basic pore models: (a) cylindrical, (b) ink-bottled and (c) slit-shaped pores.

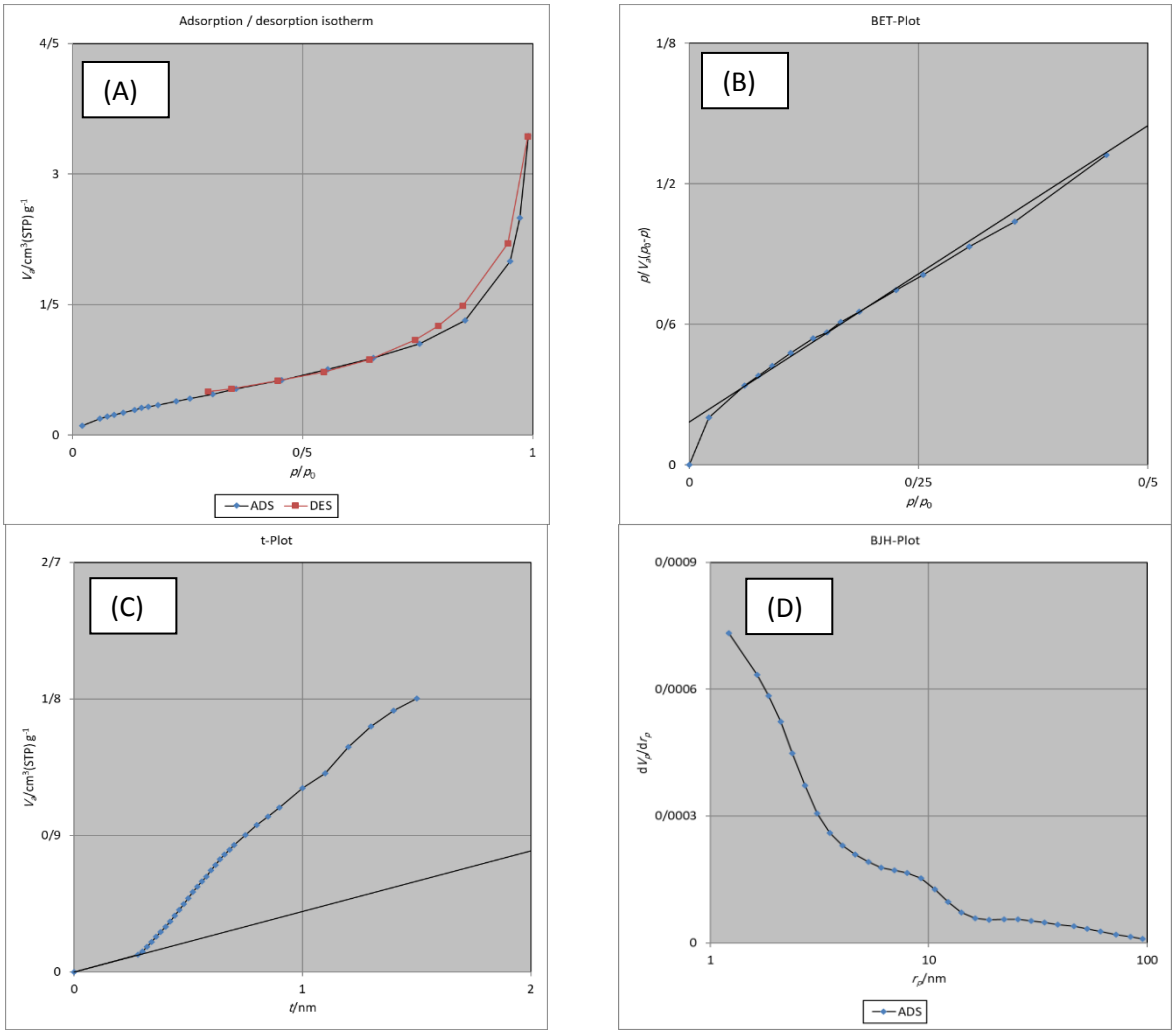

Figure 9: (A) Adsorption/desorption isotherm, (B) BET plot, (C) T plot and (D) BJH plot

Table 2
Results of porosity analysis for the 90/10 cellulose/wollastonite membrane with 100 μm thickness

Parameter	BET plot	
V_m	0.3686	[cm^3(STP) g^{-1}]
$a_{s, BET}$	1.6042	[m^2 g^{-1}]
C	14.754	
Total pore volume (p/p_0 = 0.990)	0.0052654	[cm^3 g^{-1}]
Mean pore diameter	13.129	[nm]
	BJH plot	
Plot data	Adsorption branch	
V_p	0.0055036	[cm^3 g^{-1}]
$r_{p, peak}$ (*Area*)	1.21	[nm]
a_p	2.1298	[m^2 g^{-1}]

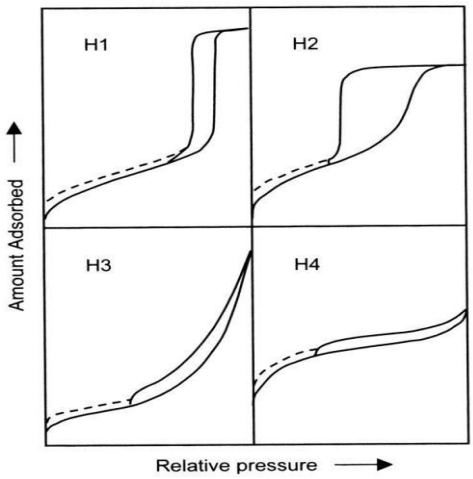

Figure 10: Relationship between pore shape and adsorption-desorption isotherm[42]

Further information about the porosity of the membrane was obtained from the isotherm data by means of BET analysis. According to the results listed in Table 2, the values of the specific surface area and the mean pore diameter obtained from the BET plot are 1.6042 m^2 g^{-1} and 13.129 nm, respectively. According to the classification proposed by IUPAC, materials with intermediate pore sizes, between 2.0 and 50.0 nm, are mesoporous. Thus, judging by these results, the membrane prepared in this study clearly presents mesopores.

The correlation between the shape of the hysteresis loop and the texture of porous materials, namely, their pore size and geometry *etc*., has been generally acknowledged (Fig. 10).[42] According to the IUPAC classification, type H_1 hysteresis is often associated with porous materials consisting of well-defined cylindrical-like pore channels or agglomerates of approximately uniform spheres. Type H_2 is ascribed to materials that are often disordered, where the distribution of pore size and shape is not well-defined and also indicative of bottleneck constrictions. Materials that give rise to H_3 hysteresis have slit-shaped pores (the isotherms revealing type H_3 do not show any limiting adsorption at high P/Po, which is observed with non-rigid aggregates of plate-like particles). The desorption curve of H_3 hysteresis contains a slope associated with a force on the hysteresis loop, due to the so-called tensile strength effect (this phenomenon occurs perhaps for nitrogen at 77 K in the relative pressure range from 0.4 to 0.45). On the other hand, type H_4 hysteresis is also often associated with narrow slit pores.[42]

The shape of the hysteresis loop was most likely caused by capillary condensation taking place in the mesoporous structures. From the data obtained from BET analysis and by comparing the adsorption-desorption curves in Figures 9 and 10, it can be concluded that the cellulose/wollastonite membranes prepared in this work are mesoporous and give rise to H_3 hysteresis, therefore have slit-shaped pores. Thus, the obtained membranes can be suggested for nanofiltration.[30]

CONCLUSION

Cellulose/wollastonite films for membrane application were successfully prepared through a simple and environmentally friendly process from N-methylmorpholine N-oxide, using an automatic film coater doctor blade, on a polyester support layer. It was observed that the porosity and pore size of the cellulose/wollastonite membrane decreased with lower cellulose and higher wollastonite amounts. The membranes became more brittle with increasing amounts of wollastonite, while pure cellulose membranes do not have enough strength to be placed on the polyester support layer. The thickness of the solution cast on the support layer also affects the membrane's porosity, specifically, too high thickness reduces porosity, while too low thickness reduces the membrane's performance.

According to BET analysis, the specific surface area and the mean pore diameter determined for the prepared cellulose/wollastonite membrane are 1.6042 m^2 g^{-1} and 13.129 nm, respectively. Thus, obtained material is a mesoporous membrane with slit-shaped pores. The presence of mesopores in the membrane indicates it can be applied in nanofiltration processes.

REFERENCES

[1] N. V. Hung, in "Sustainable Rice Straw Management", edited by M. Gummert, N. Van Hung, P. Chivenge and B. Douthwaite, Springer, 2020, pp. 165-166

[2] J. Yan, J. Liu, Y. Sun, G. Song, D. Ding *et al*., *Polymers*, **13**, 3463 (2021), https://doi.org/10.3390/polym13203463

[3] D. Roy, M. Semsarilar, J. T. Guthriea and S. Perrier, *Chem. Soc. Rev*., **38**, 2046 (2009), https://doi.org/10.1039/B808639G

[4] G. Szekely, M. F. Jimenez-Solomon, P. Marchetti, J. F. Kim and A. G. Livingston, *Green Chem*., **16**, 4440 (2014), https://doi.org/10.1039/C4GC00701H

[5] M. Ichwan and T. W. Son, *J. Appl. Polym. Sci*., **124**, 1409 (2012), https://doi.org/10.1002/app.35104

[6] R. P. Sreekanth Chakradhar, B. M. Nagabhushana, G. T. Chandrappa, K. P. Ramesh and J. L. Rao, *Mater. Chem. Phys*., **95**, 169 (2006), https://doi.org/10.1016/j.matchemphys.2005.06.002

[7] N. Zhang, J. A. Molenda, S. Mankoci, X. Zhou, W. L. Murphy *et al*., *Biomater. Sci*., **1**, 1101 (2013), https://doi.org/10.1039/C3BM60034C

[8] V. Swamy and L. S. Dubrovinsky, *Geochim. Cosmochim. Acta*, **61**, 1181 (1997), https://doi.org/10.1016/S0016-7037(96)00403-6

[9] E. Essene, *Contrib. Mineral. Petrol*., **45**, 247 (1974), https://doi.org/10.1007/BF00383442

[10] A. Yazdani, H. R. Rezaie and H. Ghassai, *J. Ceram. Process. Res.*, **11**, 348 (2010)

[11] H. Ismail, R. Shamsudin, M. A. A. Hamid and R. Awang, *J. Aust. Ceram. Soc*., **52**, 163 (2016)

[12] K. Lin, J. Chang, G. Chen, M. Ruan and C. Ning, *J. Cryst. Growth*, **300**, 267 (2007), https://doi.org/10.1016/j.jcrysgro.2006.11.215

[13] R. Abdul Rashid, R. Shamsudin, M. A. A. Hamid and A. Jalar, *J. Asian Ceram. Soc*., **2**, 77 (2014), https://doi.org/10.1016/j.jascer.2014.01.010

[14] M. M. Shukur, E. A. Al-Majeed and M. M. Obied, *Int. J. Eng. Tech*., **4**, 426 (2014)

[15] S. Vichaphund, M. Kitiwan, D. Atong and P. Thavorniti, *J. Eur. Ceram. Soc*., **31**, 2435 (2011)

[16] M. Mehrali, S. F. Seyed Shirazi, S. Baradaran, H. S. C. Metselaar, N. A. B. Kadri *et al*., *Ultrason. Sonochem*., **21**, 735 (2014), https://doi.org/10.1016/j.ultsonch.2013.08.012

[17] J. P. Nayak, S. Kumar and J. Bera, *J. Non-Cryst. Solids*, **356**, 1447 (2010), https://doi.org/10.1016/j.jnoncrysol.2010.04.041

[18] N. S. C. Zulkifli, I. Ab Rahman, D. Mohamad and A. Husein, *Ceram. Int.*, **39**, 4559 (2013), https://doi.org/10.1016/j.ceramint.2012.11.052

[19] M. Noushad, I. Ab Rahman, N. S. Che Zulkifli, A. Husein and D. Mohamad, *Ceram. Int*., **40**, 4163 (2014), https://doi.org/10.1016/j.ceramint.2013.08.073

[20] Y. H. Yun, S. B. Kim, B. A. Kang, Y. W. Lee, J. S. Oh *et al*., *J. Mater. Process. Technol*., **178**, 61 (2006)

[21] X. Wan, C. Chang, D. Mao, L. Jiang and M. Li, *Mater. Sci. Eng. C*, **25**, 455 (2005), https://doi.org/10.1016/j.msec.2004.12.003

[22] X. Jie, Y. Cao, J. J. Qin, J. Liu and Q. Yuan, *J. Membr. Sci*., **246**, 157 (2005), https://doi.org/10.1016/j.memsci.2004.08.007

[23] E. Maia, A. Peguy and S. Perez, *Acta Cryst*., **B37**, 1858 (1981)

[24] W. Berger, M. Keck and B. Philipp, *Cellulose Chem. Technol*., **22**, 387 (1988), https://www.cellulosechemtechnol.ro/

[25] E. M. Andresen and G. R. Mitchell, *Polymer*, **39**, 7127 (1998).

[26] H. Chanzy, M. Dube and R. H. Marchessault, *J. Polym. Sci. Polym. Lett*., **17**, 219 (1979)

[27] H. Strathmann, L. Giorno and E. Drioli, "An Introduction to Membrane Science and Technology", Institute of Membrane Technology, University of Calabria, 2006

[28] R. W. Baker, "Membrane Technology and Applications", Wiley, Menlo Park, California, USA, 2004
[29] K. S. W. Sing, D. H. Everett, R. A. W. Haul, L. Mouscou, R. A. Pierotti *et al*., *Pure Appl. Chem*., **57**, 603 (1985)
[30] E. Drioli and L. Giorno, "Encyclopedia of Membranes", Springer-Verlag, Heidelberg, 2016
[31] L. Feng, Y. Gao, Z. Dai, H. Dan, F. Xiao *et al*., *J. Hazard. Mater*., **415**, 125594 (2021), https://doi.org/10.1016/j.jhazmat.2021.125594
[32] A. Bhatnagar, *Master of Science Thesis*, University of Toronto, 2004
[33] W. Chen, H. Yu, Y. Liu, P. Chen, M. Zhang *et al*., *Carbohyd. Polym*., **83**, 1804 (2011)
[34] Md. N. Islam Setu, Md. Y. Mia, N. J. Lubna and A. Asad Chowdhury, *Dhaka Univ. J. Pharm. Sci*., **13**, 187 (2014)
[35] O. A. Battista, *Ind. Eng. Chem*., **42**, 502 (1950)
[36] S. Saravanan, S. Vimalraj, M. Vairamani and N. Selvamurugan, *Biomed. Nanotechnol*., **11**, 1124 (2015), https://doi.org/10.1166/jbn.2015.2057
[37] S. Azeena, N. Subhapradha, N. Selvamurugan, S. Narayan, N. Srinivasan *et al*., *Mater. Sci. Eng. C*, **71**, 1156 (2017), https://doi.org/10.1016/j.msec.2016.11.118
[38] H. M. Shaikh, A. Anis, A. M. Poulose, S. M. Al-Zahrani, N. A. Madhar *et al*., *Polymers*, **13**, 1893 (2021), https://doi.org/10.3390/polym13111893
[39] A. Azizi, *J. Inorg. Organomet. Polym. Mater*., **30**, 3552 (2020), https://doi.org/10.1007/s10904-020-01500-1
[40] R. Lakshmi and S. Sasikumar, *Int. J. Nanomed*., **10**, 129 (2015), https://doi.org/10.2147/IJN.S79986
[41] P. Kumar, B. S. Dehiya, A. Sindhu, R. Kumar, C. I. Pruncu *et al*., *Mater. Des*., **195**, 109026 (2020), https://doi.org/10.1016/j.matdes.2020.109026
[42] Z. A. Alothman, *Materials*, **5**, 2874 (2012), https://doi.org/10.3390/ma5122874